



Contents lists available at ScienceDirect

Bioorganic & Medicinal Chemistry Letters

journal homepage: www.elsevier.com/locate/bmcl

GDC-0449—A potent inhibitor of the hedgehog pathway

Kirk D. Robarge^{a,*}, Shirley A. Brunton^b, Georgette M. Castanedo^a, Yong Cui^a, Michael S. Dina^a, Richard Goldsmith^a, Stephen E. Gould^c, Oivin Guichert^c, Janet L. Gunzner^a, Jason Halladay^a, Wei Jia^a, Cyrus Khojasteh^a, Michael F. T. Koehler^a, Karen Kotkow^c, Hank La^a, Rebecca L. LaLonde^a, Kevin Lau^a, Leslie Lee^a, Derek Marshall^a, James C. Marsters Jr.^a, Lesley J. Murray^a, Changgeng Qian^c, Lee L. Rubin^c, Laurent Salphati^a, Mark S. Stanley^a, John H. A. Stibbard^b, Daniel P. Sutherlin^a, Savita Ubhayaker^a, Shumei Wang^a, Susan Wong^a, Minli Xie^a

^a Genentech, Small Molecule Drug Discovery 1 DNA Way, South San Francisco, CA 94080, United States

^b Evotec, 114 Milton Park, Abingdon, Oxfordshire OX14 4RX, United Kingdom

^c Curis Inc., 45 Moulton Street, Cambridge, MA 02138-1118, United States

ARTICLE INFO

Article history:

Received 10 July 2009

Revised 9 August 2009

Accepted 11 August 2009

Available online 15 August 2009

Keywords:

GDC-0449

Hedgehog pathway

Small molecule inhibitor

ABSTRACT

SAR for a wide variety of heterocyclic replacements for a benzimidazole led to the discovery of functionalized 2-pyridyl amides as novel inhibitors of the hedgehog pathway. The 2-pyridyl amides were optimized for potency, PK, and drug-like properties by modifications to the amide portion of the molecule resulting in **31** (GDC-0449). Amide **31** produced complete tumor regression at doses as low as 12.5 mg/kg BID in a medulloblastoma allograft mouse model that is wholly dependent on the Hh pathway for growth and is currently in human clinical trials, where it is initially being evaluated for the treatment of BCC.

© 2009 Elsevier Ltd. All rights reserved.

The focus of cancer research has shifted in recent years from agents that act on rapidly dividing cells to molecules that target specific proteins and pathways that are misregulated in tumors. Molecules acting with such specificity are potentially less toxic to normal cells that do not rely on these pathways to survive, while maintaining or improving efficacy. One subset of these oncology targets involves genes ordinarily active during embryonic development which are abnormally reactivated in adults through sporadic mutation. This reactivation can lead to tumor growth.

In the case of the Hedgehog (Hh) pathway, the 12 transmembrane receptor patched (PTCH) is a negative regulator of the seven transmembrane receptor smoothened (SMO). PTCH is the receptor for the Hh ligand and inhibits SMO until the Hh ligand binds, allowing SMO to signal. Through an intracellular pathway that is still incompletely understood, this signaling event results in the nuclear translocation of the Hh transcription factors Gli1 and Gli2, which initiate transcription of Hh responsive genes (Fig. 1).^{1,2} During development, this pathway is responsible for embryonic patterning in a variety of tissues. In patients afflicted with Gorlin Syndrome, a mutation of the negative regulator, PTCH,

causes uncontrolled SMO signaling producing multiple basal cell carcinomas (BCC)^{3,4} along with much higher growth rates of other cancers. There is also strong evidence linking alterations in the Hh pathway to sporadic BCC,^{5,6} medulloblastoma,^{7,8} small cell lung,⁹ and gastro-intestinal tract cancers,¹⁰ among others.

The Hh pathway has been studied extensively using the natural product cyclopamine, a steroidal alkaloid that blocks Hh signaling with an EC₅₀ of approximately 300 nM and has been shown to bind SMO,¹¹ to modify Hh pathway activation in cell cultures,¹² and to inhibit the proliferation of human medulloblastoma⁸ and basal cell

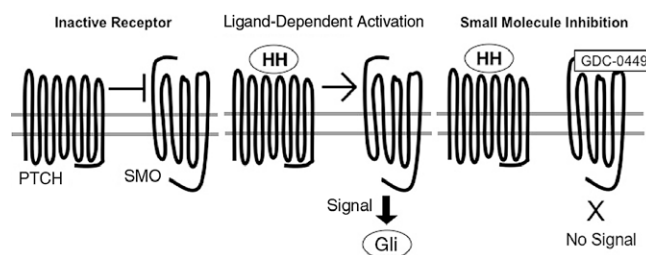


Figure 1. Diagram of Hedgehog signaling.

* Corresponding author. Tel.: +1 650 225 2320.

E-mail address: kir@gene.com (K.D. Robarge).

carcinoma¹³ skin explants. However, cyclopamine has limitations as a viable therapeutic agent. Its structural complexity, scarcity, poor aqueous solubility, and poor chemical stability in acid led us to identify small molecule Hh antagonists of a different chemical class.

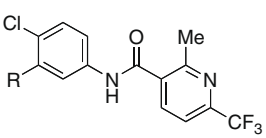
A high-throughput screen was performed based on murine 10T1/2 (S12) embryonic fibroblast cells containing a plasmid with a luciferase reporter gene downstream of Gli binding sites. When these cells are stimulated with Sonic Hh (Shh), the luciferase activity can be measured optically. Hh pathway antagonists reduce the magnitude of this signal.^{13–15} Hit-to-lead optimization of the screening hits produced benzimidazole **1** (Table 1), which had attractive potency in a Hh pathway assay. Others have reported

that a structurally similar benzimidazole antagonist of the Hh pathway displaces fluorescently labeled cyclopamine from SMO,¹⁶ leading us to believe that **1** might act in a similar fashion.

Compound **1** had several important weaknesses as a drug candidate. A primary concern was its poor metabolic stability in dogs that tracked with the high predicted clearance (22 mL/min/kg) from incubation with dog liver microsomes (Table 3) coupled with a high predicted clearance in human (9.4 mL/min/kg) from incubation with human microsomes. Additionally, the aqueous solubility was low at 0.3 µg/mL at pH 6.5. We began our investigation by targeting a wide variety of replacements for the benzimidazole, reasoning that we could rapidly modify the amide portion of any promising cores.

Two key intermediates enabled the synthesis of the majority of our heterocyclic replacements. 2-Chloro-5-nitro-acetophenone was obtained from the nitration of 2-chloroacetophenone and then converted to the α -bromo ketone to produce imidazothiazole **9**,

Table 1
SAR exploring heterocycle replacements



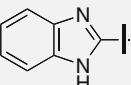
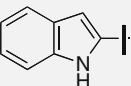
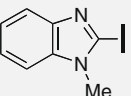
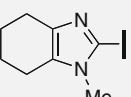
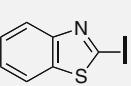
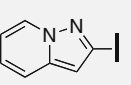
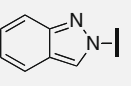
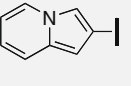
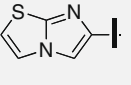
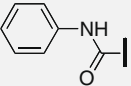
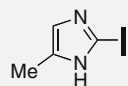
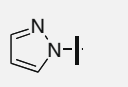
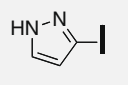
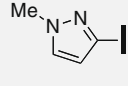
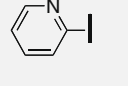
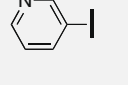
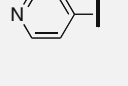
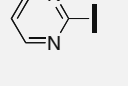
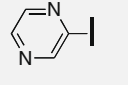
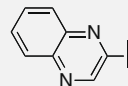
Entry	R	Gli LUC S12 IC ₅₀ (µM)
1		0.012
2		0.500
3		0.009
4		0.150
5		0.070
6		0.170
7		0.080
8		4.200
9		0.200
10		0.140

Table 1 (continued)

Entry	R	Gli LUC S12 IC ₅₀ (µM)
11		0.256
12		0.450
13		9.000
14		0.550
15		0.042
16		10.00
17		2.400
18		8.000
19		1.700
20		0.052

pyrazine **19**, and quinoxaline **20** (Scheme 1). Formation of indolizine **8** required initial reduction of the nitro and coupling of the 2-methyl-6-trifluoromethyl nicotinic acid portion before the heterocycle could be formed.

A second group of benzimidazole replacements were synthesized from 2-chloro-5-nitroaniline, which was converted to the isomeric pyridines **15**, **16**, and **17** as well as the pyrimidine **18** (Scheme 2) through conversion of the aniline to a halogen and subsequent coupling to the desired heterocycle. Alternatively, diazotization and reduction to the corresponding hydrazine gave rise to the pyrazole in **12**. The indazole in **7** was obtained by forming an imine with 2-nitrobenzaldehyde and subsequent reduction of the adjacent nitro group. Compounds **7**, **12**, **15**, and **17** were obtained through reduction of the aryl nitro group and subsequent acylation.

Benzimidazoles **1** and **3** and the reduced benzimidazole **4** were accessed via 2-chloro-5-nitrobenzoyl chloride (Scheme 3), as was the ring opened amide analog **10**. Finally, pyrazolopyridine **6** was synthesized by cyclization of aminopyridinium iodide with the acrylate obtained from 2-chloro-5-nitrobenzaldehyde followed by decarboxylation and rearomatization (Scheme 4).

Following their synthesis, potencies were determined in the Gli luciferase assay. The clearest trend emerging from the resulting SAR (Table 1) was a preference for a hydrogen bond acceptor to be adjacent to the ring junction. When the benzimidazole in **1** was replaced with the isosteric indole in compound **2**, which lacks a hydrogen bond acceptor, potency dropped more than 40-fold. At the same time, methylation of the benzimidazole nitrogen to remove a hydrogen bond donor adjacent to the ring junction in compound **3** did not affect potency significantly. Other potent bicycles which follow this SAR trend include thiazole **5** and quinoxaline **20**. Additionally, amide **10** can be seen as following this same trend with the carbonyl oxygen serving as the hydrogen bond acceptor.

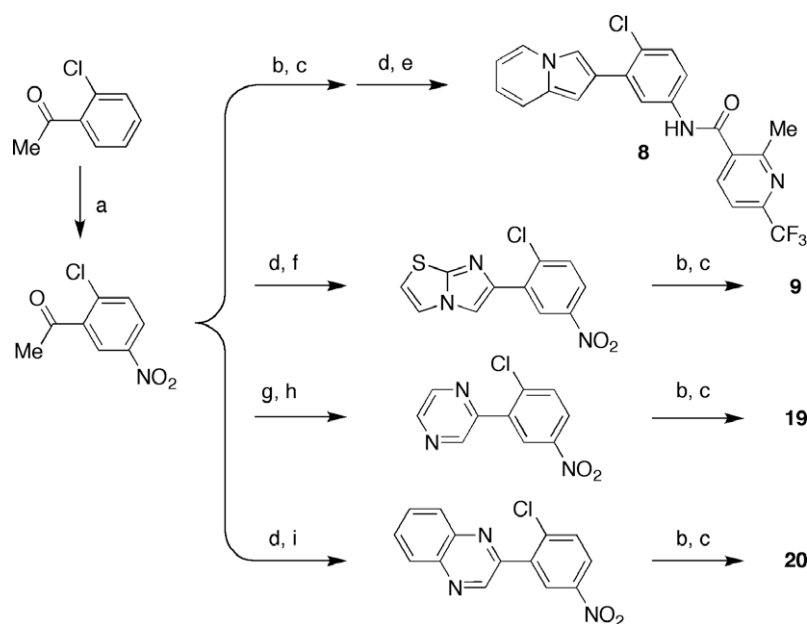
Both indazole **7** and pyrazolopyridine **6** are less potent than the isosteric benzimidazole **1** likely due to the reduced basicity of the key nitrogen adjacent to the ring. pK_a values for this nitrogen in **6** and **7** were calculated to be -0.28 and -0.79 , respectively, while

that of **1** was 4.16 .¹⁸ The requirement for a basic nitrogen adjacent to the ring fusion is also observed in the single ring replacements for the benzimidazole. The only single ring replacement for the benzimidazole with an IC_{50} less than 50 nM is the 2-pyridyl compound **15**. As would be predicted from the bicyclic analogs, the regioisomeric 3- and 4-pyridines **16** and **17** were significantly less potent. Pyrazole **12** showed only moderate potency, which was greatly reduced in the regioisomeric **13**, presumably because one of its tautomeric forms cannot serve as a hydrogen bond acceptor. When the pyrazole is methylated, as in **14**, preventing the tautomerization, the potency is restored.

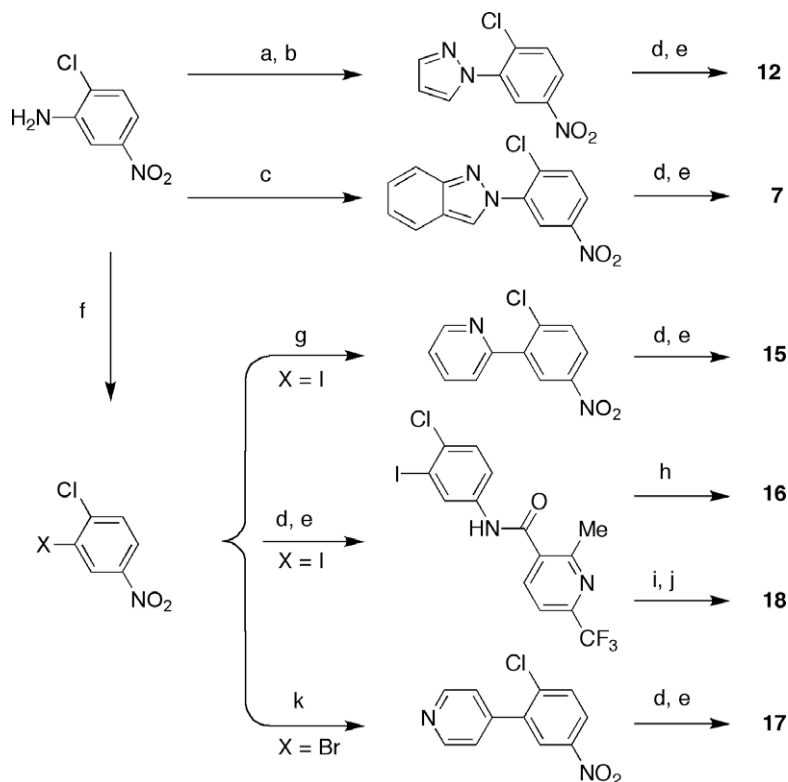
The second trend in the SAR was a preference for an aromatic ring fused to the nitrogen containing heterocycle. Imidazole **11**, for example, is greater than 20-fold less potent than the corresponding benzimidazole **1**. Similarly, the saturated tetrahydrobenzimidazole **4** was found to be almost 17-fold less potent than **3** and pyrazine **19** is 32-fold less potent than quinoxaline **20**.

Having developed a group of possible replacements for the benzimidazole portion of the molecule, we sought to optimize the amide portion of our biaryls. Compound **3** was the most potent but was not further considered due to moderate CYP inhibition against 2C9 ($IC_{50} = 2.5$ μ M) and 4.3–6-fold higher in vivo clearance in rat compared to **15** and **1**. Of our most potent heterocycles, we chose compound **15** as a starting point due to its superior PK in dog compared to **1** (Table 3). Additionally the predicted clearance of **15** was lower than that of indazole **7** and quinoxaline **20** in the preclinical species examined and tracked with in vivo clearance. Quinoxaline **20** also exhibited improved PK in dog versus **1** but had poor solubility.

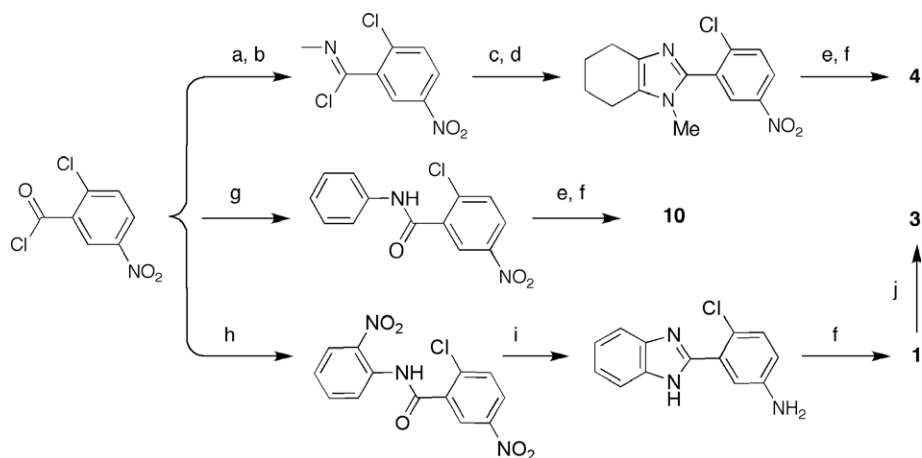
After examining a wide variety of amide substituents, several broad themes emerged (Table 2). It appears beneficial to have a lipophilic substituent in the 2-position of the ring such as a chloro or methyl substituent as in compounds **15**, **21**, and **26**. The Cl/Me groups may be making a hydrophobic contact with the protein or forcing the aromatic ring out of plane with the amide bond.¹⁹ Moving the chloro atom to other ring positions decreased the potency as evidenced in amides **27** and **28** when compared to the amide **26**.



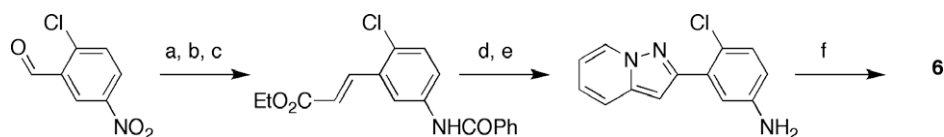
Scheme 1. Reagents and conditions: (a) HNO_3 , H_2SO_4 ; (b) Fe, HOAc; (c) 2-methyl-6-trifluoromethyl-3-nicotinic acid, EDC, 6-Cl HOBt, DIPEA, DMF or 2-methyl-6-trifluoromethyl-3-nicotinoyl chloride, CH_2Cl_2 , DIPEA, $0^\circ C$, 2 h; (d) Br_2 , $HBr/AcOH$, benzene, $0^\circ C$; (e) acetone, 2-methylpyridine, K_2CO_3 ; (f) 2-aminothiazole, EtOH; (g) 48% HBr , DMSO; (h) ethylene diamine, MnO_2 , C_6H_6 , reflux; (i) phenylenediamine, NaOAc, EtOH, air.



Scheme 2. Reagents and conditions: (a) HCl, NaNO₂, then SnCl₂; (b) malonaldehyde bis(diethyl acetal), EtOH; (c) 2-nitrobenzaldehyde, POEt₃; (d) Fe, HOAc, 80 °C, 0.5 h or SnCl₂, EtOH, concd HCl; (e) 2-methyl-6-trifluoromethyl-3-nicotinoyl chloride, CH₂Cl₂, DIPEA, 0 °C, 2 h; (f) NaNO₂; KI (g) 2-pyridyl zinc iodide in THF, Pd(PPh₃)₄, TFP, CuI, DMA; (h) 3-pyridyl boronic acid pinacol ester, Pd(PPh₃)₄, K₂CO₃, 4:1 Tol/EtOH, 0.15 h microwave; (i) pinacol diborane, PdCl₂(dppf), DMF, 130 °C, 0.4 h microwave; (j) 2-bromopyrimidine, Pd(PPh₃)₄, K₂CO₃, 4:1 Tol/EtOH, 160 °C, 0.2 h microwave; (k) 4-pyridyl boronic acid pinacol ester, Pd(PPh₃)₄, K₂CO₃, 4:1 Tol/EtOH, 160 °C, 0.2 h microwave.

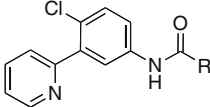
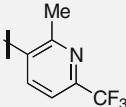
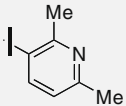
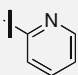
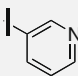
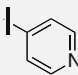
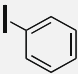
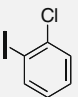
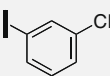
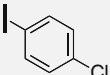
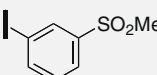
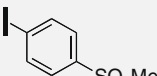
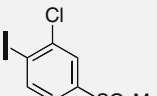


Scheme 3. Reagents and conditions: (a) toluene, H₂NMe, 2.0 M in THF, 0 °C, 1.5 h; (b) SOCl₂, neat, reflux 1.5 h; (c) *N*-Me carboxyimidazole chloride, THF, TEA, cyclohexanone oxime, THF, −70 °C to rt;¹⁷ (d) *p*-toluenesulfonic acid, toluene, Dean Stark, reflux 2 d; (e) Fe, HOAc, 80 °C, 0.5 h; (f) DIPEA, CH₂Cl₂, 2-methyl-6-trifluoromethyl-3-nicotinoyl chloride, 0 °C, 2 h; (g) DIPEA, CH₂Cl₂; (h) 2-nitroaniline, pyridine, CH₂Cl₂; (i) zinc, acetic acid; ethylene glycol, KOH; (j) MeI, acetone, NaOH.



Scheme 4. Reagents and conditions: (a) (ethoxycarbonylmethylidene) triphenylphosphorane, toluene, 50 °C; (b) Fe, AcOH, EtOH; (c) benzoyl chloride, Et₃N, CH₂Cl₂; (d) 1-aminopyridinium iodide, K₂CO₃, DMF 40 °C (e) H₂SO₄, H₂O; (f) 2-methyl-6-trifluoromethyl-3-nicotinoyl chloride, CH₂Cl₂, DIPEA, 0 °C, 2 h.

Table 2
SAR exploring amide group substituents

		
Entry	R	Gli LUC S12 IC ₅₀ (μM)
15		0.042
21		0.130
22		3.000
23		0.600
24		0.700
25		0.800
26		0.110
27		1.500
28		1.500
29		0.120
30		0.040
31		0.013

The aromatic nitrogen in **15** appears to play almost no role in its potency. Picolinic amide **22** displayed reduced potency relative to **25**, while the nicotinic and isonicotinic amides **23** and **24** were essentially equipotent with **25**. We speculate that having a nitrogen in the 2-position may reduce potency by enforcing coplanarity between the amide and aryl ring through an internal hydrogen bond. The presence of a sulfonyl group in the 3- or 4-position had a positive effect on binding as demonstrated by **29** and **30**, with the 4-position preferred.

Having optimized the potency and metabolic stability, solubility became our primary concern. Methylsulfone **30** was equipotent with nicotinic amide **15** and possesses a lower cLog *P* but did not improve the solubility at pH 6.5 (Table 3). At this point, an *o*-chloro group, added to enhance potency, was found to significantly improve the solubility at neutral pH. The nearly 20-fold improvement from **30** to **31** occurs despite a predicted increase in clog *P*, and may reflect the reduced planarity of the aryl amide. This does not however result in a decreased melting point for **31** (264 °C) as it was measured to be very similar to **30** (251 °C, both measured as crystalline HCl salts).

The resulting compound **31** (GDC-0449) exhibited improved potency, solubility and metabolic stability relative to **15** or **30** (Table 3). This compound was also potent (2.8 nM) in an analogous human Gli luciferase assay using human embryonic palatal mesenchyme (HEPM) cells.

Compounds **15**, **30**, and **31** possess excellent potency and low clearance in both rats and dogs. Low clearance combined with high absorption translated to high oral exposures.²⁰ Compounds **15** and **31** also demonstrated improved solubility at pH 6.5 relative to others in this series. To further characterize these compounds, a PK/PD study was performed using the Hh responsive tumor cell line CALU-6 in nude mice.

The CALU-6 cell line is known to recruit a large stromal component, where Hh signaling appears to be operative in tumorigenesis.²¹ Nude mice implanted with human CALU-6 cells were orally dosed with 75 mg/kg BID of compound **15**, **30**, or **31** for 3 days to allow complete suppression of Hh signaling to develop. Following the final dose, the amount of Gli transcription in the stroma was determined with mouse specific primers and correlated with exposure (Fig. 2). The nicotinic amide **15** was unable to achieve high enough exposure to see a significant amount of knock down at 4 h post fifth dose, possibly due to solubility limited absorption at this higher dose. The unsubstituted methyl sulfone **30** fared slightly better but displayed a large degree of variability from animal to animal, again possibly due to poor solubility. The more soluble chloromethylsulfone **31** exhibited a greater than 10-fold knock-down of Gli suppression versus control and reduced variability. We attribute the greater degree of Gli suppression to higher plasma concentrations, increased potency and a higher free fraction (9% free vs 3% (**30**)).

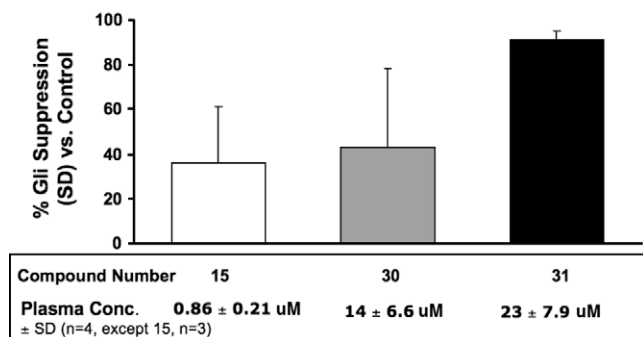
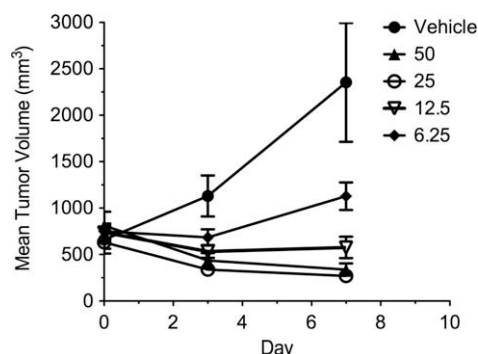
Compound **31** was explored further in a Hh pathway dependent medulloblastoma allograft model generated from Ptch^{+/-} mice²² and produced complete regression at doses as low as 12.5 mg/kg BID (Fig. 3). In addition to the mutation-driven autocrine signaling medulloblastoma model, Hh antagonists have been shown to delay growth in primary human tumor xenograft models.²¹

Having started from the potent lead compound **1**, we investigated a diverse set of heterocyclic replacements for the benzimidazole. This led to a potent series of 2-pyridyl biaryls, which were further optimized for potency, metabolic stability, PK, and drug-like properties by incorporating the *p*-methyl sulfone and *o*-chloro functionalities in the amide portion of the molecule. This resulted in the discovery of Hh antagonist **31**, which has progressed into human clinical trials, where it is being initially evaluated in the treatment of BCC. Since the initiation of GDC-0449 clinical trials, other Hh pathway inhibitors have entered early stage clinical testing and

Table 3

Pharmacokinetics in preclinical species

Entry	Potency Gli LUC S12 IC ₅₀ (nM)	CL (hep) pred. from microsomes (mL/min/kg)			Measured clearance (mL/min/kg)		cLog P	Solubility (μg/mL)	
		Rat	Dog	Human	Rat	Dog		pH 1.0	pH 6.5
1	12	18.5	22	9.4	3.0	124	3.9	300	0.3
7	80	32	17	7.6	99.3	NA	3.8	NA	NA
20	52	9.1	16	7.4	10.7	7.4	4.1	0.1	0.1
15	42	5.9	10	0.6	4.5	1.9	3.7	1000	1.8
30	40	2.8	11	5.9	1.2	1.4	3.2	420	0.5
31	13	3.7	11	4.5	3.7	0.4	4.0	>3000	9.5

**Figure 2.** Gli suppression measured in CALU-6 tumors grown in nude mice. Plasma levels of **15**, **30**, and **31** were measured at the time of tumor harvest, 4 h after the fifth dose.**Figure 3.** Ptch +/- medulloblastoma allografts treated orally with GDC-0449 formulated as a suspension in 0.5% methylcellulose, 0.2% Tween-80 (MCT).²³

several more discovered over the last decade are in pre-clinical development.²⁴

Acknowledgments

The authors thank Martin Struble and Mengling Wong for purification of compounds, Vickie Tsui for computational support, Harvey Wong for transport studies with GDC-0449, and Mike Reich and the in vivo group for their support of PK and PK/PD studies.

References and notes

- Rubin, L. L.; de Sauvage, F. J. *Nat. Rev. Drug Disc.* **2006**, *5*, 1026.
- Stone, D. M.; Hynes, M.; Armanini, M.; Swanson, T. A.; Gu, Q.; Johnson, R. L.; Scott, M. P.; Pennica, D.; Goddard, A.; Phillips, H.; Noll, M.; Hooper, J. E.; de Sauvage, F.; Rosenthal, A. *Nature* **1996**, *384*, 129.
- Hahn, H.; Wickin, C.; Zaphiropoulos, P. G.; Gailani, M. R.; Shanley, S.; Chidambaram, A.; Vorechovsky, I.; Holmberg, E.; Uden, A. B.; Gillies, S.; Negus, K.; Smyth, I.; Pressman, C.; Leffell, D. J.; Gerrard, B.; Goldstein, A. M.; Dean, M.; Toftgard, R.; Chenevix-Trench, G.; Wainwright, B.; Bale, A. E. *Cell* **1996**, *85*, 841.
- Johnson, R. L.; Rothman, A. L.; Xie, J.; Goodrich, L. V.; Bare, J. W.; Bonifas, J. M.; Quinn, A. G.; Myers, R. M.; Cox, D. R.; Epstein, E. H.; Scott, M. P. *Science* **1996**, *272*, 1668.
- Dahmane, N.; Lee, J.; Robins, P.; Heller, P.; Ruiz I Altababa, A. *Nature* **1997**, *389*, 876.
- Xie, J.; Murone, M.; Luoh, S. M.; Ryan, A.; Gu, Q.; Zhang, C.; Bonifas, J. M.; Lam, C. W.; Hynes, M.; Goddard, A.; Epstein, E. H., Jr.; de Sauvage, F. J. *Nature* **1998**, *391*, 90.
- Raffel, C.; Jenkins, R. B.; Frederick, L.; Hebrink, D.; Alderete, B.; Fults, D. W.; James, C. D. *Cancer Res.* **1997**, *57*, 842.
- Berman, D. M.; Karhadkar, S. S.; Hallahan, A. R.; Pritchard, J. I.; Eberhart, C. G.; Watkins, D. N.; Chen, J. K.; Cooper, M. K.; Taipale, J.; Olson, J. M.; Beachy, P. A. *Science* **2002**, *297*, 1559.
- Watkins, D. N.; Berman, D. M.; Burkholder, S. G.; Wang, B.; Beachy, P. A.; Baylin, S. B. *Nature* **2003**, *422*, 313.
- Berman, D. M.; Karhadkar, S. S.; Maitra, A.; Montes de Oca, R.; Gerstenblith, M. R.; Briggs, K.; Parker, A. R.; Shimata, Y.; Eshleman, J. R.; Watkins, D. N.; Beachy, P. A. *Nature* **2003**, *425*, 846.
- Chen, J. K.; Taipale, J.; Cooper, M. K.; Beachy, P. A. *Genes Dev.* **2002**, *16*, 2743.
- Cooper, M. K.; Porter, J. A.; Young, K. E.; Beachy, P. A. *Science* **1998**, *280*, 1603.
- Williams, J. A.; Guicherit, O. M.; Zaharian, B. I.; Xu, Y.; Chai, L.; Wichterle, H.; Kon, C.; Gatachalian, C.; Porter, J. A.; Rubin, L. A.; Wang, F. Y. *PNAS* **2003**, *100*, 4616.
- Frank-Kamenetsky, M.; Zhang, X. M.; Bottega, S.; Guicherit, O.; Wichterle, H.; Dudek, H.; Bumcrot, D.; Wang, F. Y.; Jones, S.; Shulok, J.; Rubin, L. L.; Porter, J. A. *J. Biol.* **2002**, *1*, 10.
- Brunton, S. A.; Stibbard, J. H. A.; Rubin, L. L.; Kruse, L. I.; Guicherit, O. M.; Boyd, E. A.; Price, S. J. *Med. Chem.* **2008**, *51*, 1108.
- Chen, J. K.; Taipale, J.; Young, K. E.; Maiti, T.; Beachy, P. A. *PNAS* **2002**, *99*, 14071.
- Lantos, I.; Zhang, W. Y.; Shui, X.; Eggleston, D. S. *J. Org. Chem.* **1993**, *58*, 7092.
- Milletti, F.; Storch, L.; Sforza, G.; Cruciani, G. J. *Chem. Inf. Model.* **2007**, *47*, 2172.
- In a survey of the Cambridge Structural Database, the torsion profile between amides and aryl rings peak at angles around 30° and 150° for unsubstituted benzamides whereas this distribution peaks at angles of around 60° and 120° for *ortho*-chloro benzamides.
- Contrary to a recent report, GDC-0449 showed no evidence of Pgp inhibition and had no effect on digoxin transport in MDR1-MDCK cells at 15 μM. GDC-0449 may have been misidentified as HhAntag691 in this publication (Zhang, Y.; Laterra, J.; Pomper, M. G. Hedgehog Pathway Inhibitor HhAntag691 Is a Potent Inhibitor of ABCG2/BCRP and ABCB1/Pgp, *Neoplasia*, **2009**, *11*, 96).
- Yauch, R. L.; Gould, S. E.; Scales, S. J.; Tang, T.; Tian, H.; Ahn, C. P.; Marshal, D.; Fu, L.; Januario, T.; Kallop, D.; Nannini-Pepe, M.; Kotkow, K.; Marsters, J. C., Jr.; Rubin, L. L.; de Sauvage, F. J. *Nature* **2008**, *455*, 406.
- Corcoran, R. B.; Scott, M. P. *J. Neuro-Oncology* **2001**, *53*, 307.
- Mice were dosed twice daily. N=6 per group. Tumors were serially transplanted subcutaneously in female CD-1 nude mice. The HCl salt of GDC-0449 was resuspended in MCT (0.5% methylcellulose, 0.2% Tween-80).
- Tremblay, M. R.; Nesler, M.; Weatherhead, R.; Castro, C. *Expert Opin. Ther. Patents* **2009**, *19*, 1.